The Role of Wind-Generated Mixing in Coastal Upwelling

R. A. DE SZOEKE AND J. G. RICHMAN

School of Oceanography, Oregon State University, Corvallis 97331

(Manuscript received 2 April 1981, in final form 28 July 1981)

ABSTRACT

A simple parameterization of mixing processes originally developed by Kraus and Turner (1967) is included in a two-dimensional, two-layer theory of wind-driven coastal upwelling. Mixed-layer deepening is a competition between entrainment due to wind stirring, stabilization due to surface heating, and upwelling vertical velocity. For longshore winds favorable to upwelling, the temperature of the surface water mass being pushed offshore by the wind is determined by that of the incoming subsurface water mass, by the surface heating, and by the mixing dynamics. An upwelling steady state is possible with surface heating. In this state, the vertical upwelling velocity is exactly matched by the entrainment velocity, and the resulting cold water flux into the mixed layer is balanced by surface heating; surface temperature increases linearly with distance offshore. Time-dependent numerical solutions exhibit a tendency toward this steady-state solution. Winds favorable to downwelling cause detrainment of light water from the mixed layer into the quiescent lower layer, leading to conditions lacking any symmetry with those found for upwelling-favorable winds. This feature, observed in nature, is a consequence of the nonlinearity and irreversibility of the mixing processes in the theory. Computed model solutions for upwelling and downwelling bear reasonable resemblance to hydrographic observations made off Oregon during 1972 and 1973.

1. Introduction

The elements of the dynamics of wind-driven coastal upwelling have long been appreciated (Sverdrup *et al.*, 1942, p. 501). These are an offshore mass transport in a surface frictional layer driven by a longshore wind, a compensating transport in the interior or bottom frictional layer, and an upwelling region at the coast where the circuit between the interior (or bottom) and the surface layer is completed. Ekman's (1905) theory of wind-driven surface currents explained the part of the process associated with the offshore surface layer transport. Yoshida (1955) forged a link in the understanding of upwelling dynamics by advancing a vorticity argument which shows the influence of stratification on the structure of the upwelling mass circulation, and gives a scale for the width of the upwelling region, *viz.*, Rossby's (1938) radius of baroclinic deformation. An elegant theoretical model incorporating these elements was constructed by Allen (1973) using the techniques of boundary layer analysis. Both theoretical (Pedlosky, 1974, 1978a,b) and numerical models (Hurlburt and Thompson, 1973) have added to the understanding of the effects of longshore structure, bottom topography, time dependence and nonlinearity. Stratification has been modeled continuously in the vertical (Allen, 1973; Pedlosky, 1974, 1978a,b), or in the form of multiple (usually two) layers (Hurlburt and Thompson, 1973). Theories of coastal upwelling have been reviewed by Allen (1980).

A missing element in these models has been the diabatic character of the coastal upwelling circulation. When colder denser water rises near the coast, it mixes with warmer, lighter surface water, or is warmed by heat transferred from the air or both (Mooers *et al.*, 1976). To some extent this mixing can be modeled by vertical diffusion of the constant eddy-diffusivity type (Allen, 1973), although such a parameterization seems far from the character of mixing observed in nature, and is in truth little more than a mathematical fudge. The detailed mixing processes form one of the crucial elements of the dynamical picture of upwelling: they explicitly determine the nature of the water mass transformation that occurs during upwelling (Mooers *et al.*, 1976). Concomitantly, dynamically passive scalars such as nutrients and dissolved oxygen concentration are redistributed in ways that determine the biological state of the upwelling ecosystem. It is on the effects of the mechanisms of mixing that play a role in upwelling that we wish to treat in this paper.

The place that the present model takes in the evolution of coastal upwelling theory may be illustrated by contrasting it with the free inertial stratified models of Pedlosky (1978a,b) in which temperature is conserved following the motion. To counter the difficulty of adiabatically overturning stably stratified

0022-3670/81/111534-14$07.50

water in the upwelling circuit, Pedlosky (1978a) adopted the artifice of a line sink of buoyancy and mass at the surface along the coast. This line sink is presumably the link between the inertial interior and the frictional surface mixed layer, which is not explicitly treated in the model. In this paper we take an approach that is the inverse of Pedlosky's (1978a,b). We assume an extremely primitive model of the dynamics of the upwelling circulation—namely, that longshore wind stress τ^y drives an offshore flow $\tau^y/\rho f$ in the mixed layer, that this offshore flux is balanced by an onshore transport in the interior, and that, following Yoshida (1955), the circuit is completed by upwelling in a coastal region of the width of the Rossby radius of baroclinic deformation—and explore instead a parameterization of the turbulent entrainment and mixing in the surface layer.

Our starting point in the treatment of mixing is the one-dimensional mixed-layer model of Kraus and Turner (1967, hereafter referred to KT) who hypothesized that the surface layer thickens as a result of direct stirring by the wind and proposed a parameterization based on laboratory experiments (Rouse and Dodu, 1955; Turner, 1968). Pollard *et al.* (1973) proposed an alternative mixing mechanism based on turbulence production by inertial motion shear, while Niiler (1975) constructed a unified idealized model of the two processes and discussed some of its mathematical properties. De Szoeke and Rhines (1976) carried this discussion further and illustrated the time scales (rapid for inertial current shear mixing, slower for wind stirring) on which the two mechanisms operate. Price *et al.* (1978) found observational support for the shear mixing mechanism during a hurricane in the Gulf of Mexico. Our model will contain only the wind-stirring mechanism originally proposed by KT. This choice is determined partly by considerations of simplicity, but also by the experience of Denman (1973) and Denman and Miyake (1973), who achieved reasonable success in applying a KT model to simulate observed summertime conditions of the mixed layer at Ocean Station P. Similarly, Davis *et al.* (1981a,b) found that the wind-stirring mechanism adequately accounts for observations of the change of mixed-layer structure over a 19-day experiment at Ocean Station *P*—with some indication of enhanced mixing (perhaps due to shear) during two moderate storms. The inclusion of shear-generated mixing, especially by the energetic inertial motions observed by Kundu (1976) and Johnson *et al.* (1976), into our theoretical formalism must await further development for the coastal situation [cf. de Szoeke (1980), for an open ocean treatment]. Thompson (1978) presented a two-layer numerical model of coastal upwelling with parameterized entrainment and mixing. The model contains very complex dynamics which gives rise to internal Ekman layers at the two-layer interface and thereby permits complicated frictionally-balanced secondary circulation cells such as the one for which Mooers *et al.* (1976) found some observational support. Our approach in this paper is rather different, namely, to present the simplest model of entrainment and mixing processes in coastal upwelling context that we are able to devise, so that we can obtain semi-analytic solutions which can be studied for the physical insight that they afford.

We are aware that more complex models, even of one-dimensional mixed layers, exist (Mellor and Durbin, 1975; Kundu, 1980). These are continuous models in the vertical with detailed parameterizations of turbulent transport processes and dissipation. Our plea for not taking this approach is simplicity and computational tractability.

In Section 2 the coastal model, including KT mixed-layer dynamics, extended to take account of two-dimensional (normal-to-shore as well as vertical) effects is introduced. In Section 3 the existence of a steady-state solution for upwelling-favorable winds only in the case of positive surface heating is noted, while in Section 4a a demonstration of how a semi-analytical numerical time-dependent solution tends toward this steady-state is given. Turning to the effects of downwelling-favorable winds in the presence of surface heating, in Section 4b we discuss modifications to the semi-analytical solution technique that must be introduced to handle a decadent phase of mixing dynamics when the Monin-Obukhov depth scale is attained by the mixed layer and it *detrains* fluid into the lower layer; sample numerical solutions using the modified technique are presented. Section 5 contains a comparison of observations of both upwelling and downwelling events from Oregon to the respective model solutions. In Section 6 a critical discussion of the model, indicating possible directions for improvement concludes the paper.

2. The model

Consider a model consisting of two homogeneous layers of fluid of constant total depth, separated by an entraining interface and abutting a coastline (Fig. 1). Alongshore uniformity is assumed. An alongshore wind stress $\hat{y}\tau(t)$ is applied. Suppose that bulk Ekman-layer dynamics pertain to the upper layer. The time scale for adjustment of the Ekman volume transport to a varying wind is the pendulum day (Greenspan, 1968). For winds varying more slowly than this, the adjustment can be regarded as instantaneous. We take the volume transport of the upper layer to be

$$h_1 u_1 = (f\rho)^{-1}\tau(t)(1 - e^{x/\lambda}), \qquad (1a)$$

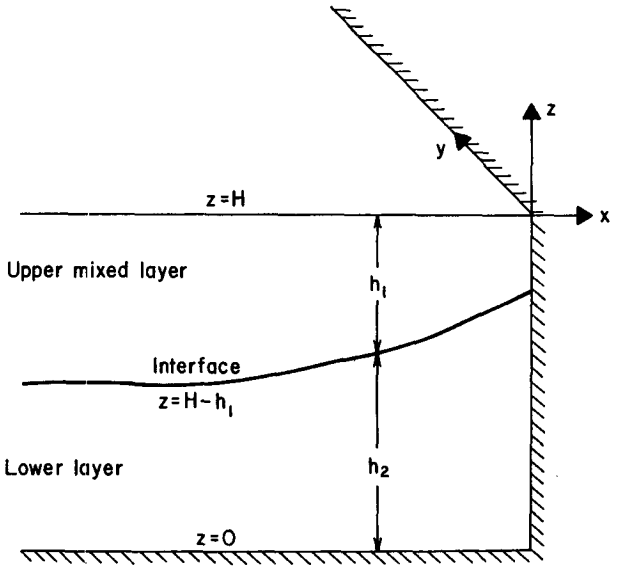

FIG. 1. Definition sketch of the model.

where f is Coriolis parameter. This reduces to the Ekman balance $h_1u_1 = \tau/f\rho$ far offshore where $-x \gg \lambda$, vanishes at the coast ($x = 0$), and passes through a smooth transition layer of width λ along the coast. This is precisely the solution arrived at by Yoshida (1955) in a two-layer model of upwelling circulation if λ is taken to be the Rossby (1938) radius of baroclinic deformation,

$$\lambda = (g\Delta\rho h)^{1/2}/f, \tag{2}$$

where h is a typical thickness of the surface mixed layer, $\Delta\rho$ is the density difference between the layers, and g is gravity. Yoshida's (1955) theory, in outline, runs as follows. In the coastal layer Coriolis force is partly balanced by longshore acceleration, or equivalently, vortex stretching is balanced by rate of change of relative vorticity. But the latter is related to the rate of elevation of internal isopycnals (or layer interface in a two-layer model) through the thermal wind relationship. In this way, stratification is called into play and introduces the Rossby deformation radius λ as a natural length scale.

Assumption (1a) evades the important question of the correct momentum dynamics of the upper mixed layer. The replacement of (1a) by a momentum balance equation consistent with the rest of the entrainment model is a goal of our continuing research. Preliminary efforts in this direction have yielded an equation whose numerical solution differs little from the heuristic solution (1a). This work will be reported in a forthcoming paper; for the present purposes, we are emboldened to persist with (1a), exploiting its simplicity and focussing attention on the novelty of the entrainment parameterization in the model. In any case, given (1a) for the volume transport in the mixed layer, its divergence $(h_1u_1)_x$ yields the motion normal to the interface at the mixed-layer base.[1] For mass balance, the transport in the lower layer must be equal and opposite to (1a), *viz.*,

$$h_2u_2 = -h_1u_1. \tag{1b}$$

The heat balance for the upper layer is

$$\frac{\partial T_1}{\partial t} + u_1\frac{\partial T_1}{\partial x} = \frac{-\partial}{\partial z}\overline{w'T'}$$

$$= \frac{1}{h_1}[-\overline{w'T'}(0) + \overline{w'T'}(-h_1)], \tag{3}$$

where $-\overline{w'T'}(0) = Q/c\rho$ is the net surface heat flux, and $-\overline{w'T'}(-h_1) = (T_1 - T_2)w_e$ is the entrainment heat flux at the interface. w_e is the entrainment velocity, given by

$$w_e = \frac{Dh_1}{Dt} + w = \frac{\partial h_1}{\partial t} + \frac{\partial}{\partial x}(h_1u_1) \tag{4}$$

(de Szoeke, 1980), where w is the vertical particle velocity just above the interface. w_e may be thought of as the difference between the particle velocity w and the apparent motion of the interface $-Dh_1/Dt$. Combining these expressions we have

$$h_1\left(\frac{\partial T_1}{\partial t} + u_1\frac{\partial T_1}{\partial x}\right)$$

$$= \frac{Q}{c\rho} - (T_1 - T_2)\left[\frac{\partial h_1}{\partial t} + \frac{\partial}{\partial x}(h_1u_1)\right]. \tag{5}$$

The lower layer temperature we assume to remain constant in time and uniform in space,

$$T_2 = \text{constant}. \tag{6}$$

An entrainment hypothesis is needed to close the system of equations. We choose

$$\left.\begin{aligned} \tfrac{1}{2}h_1\alpha g(T_1 - T_2)w_e &= m_0u_*^3 - \tfrac{1}{2}h_1\alpha gQ/c\rho \\ (u_* &= |\tau/\rho|^{1/2}) \end{aligned}\right\}, \tag{7}$$

which was first proposed for a horizontally uniform situation by KT. Discussion of this and related parameterizations appears in Denman (1973), Niiler (1975), Niiler and Kraus (1977), de Szoeke and Rhines (1976). For a generalization of the formalism to three dimensions, see de Szoeke (1980). Eq. (7) is interpreted as follows. The left side is the rate of increase of potential energy due to entrainment and mixing of colder water from the lower layer into the upper ($T_2 < T_1$), which must be equivalent energetically to raising the entrained negative buoy-

[1] Vertical velocity is $w_1 = h_1u_{1x}$ just above the mixed-layer base. The velocity normal to the interface is actually $(w_1 + u_1h_{1x})/(1 + h_{1x}^2)^{1/2} = (h_1u_1)_x/(1 + h_{1x}^2)^{1/2} \approx (h_1u_1)_x$, which is continuous across the interface (de Szoeke, 1980).

ancy anomaly $-\alpha g(T_1 - T_2)$ to the center of the mixed layer through a vertical distance $(1/2)h_1$ at the rate w_e. The first term on the right is the parameterization KT suggests for the excess of turbulent energy input by direct wind stirring at the surface over dissipation, m_0 being an empirical constant expected to be of order 1. The last term represents the stabilizing effect of surface heating, which attenuates net production $m_0 u_*^3$ (if the ocean loses heat to the atmosphere, $Q_0 < 0$, so that this term is the convective energy production term). With w_e related to change of mixed-layer depth and flow divergence by (4), effects of horizontal variation are automatically taken into account (de Szoeke, 1980). Following Davis *et al.* (1981b), we take $m_0 = 0.5$.

We have already remarked in the Introduction on alternative mechanisms, such as shear, for entrainment. Another possibility is bottom turbulence generated by strong tidal currents, which has been observed to cause vertical mixing in shallow seas (Simpson *et al.*, 1978; Pingree and Griffiths, 1978). Such mechanisms are overlooked in (7) on grounds of simplicity, not because they have been established as unimportant.

Gathering together (1), (4), (5) and (7), we have a closed system for T_1, h_1 and u_1 which could be integrated numerically given $\tau(t)$, $Q(x, t)$ and T_2. Throughout this paper τ and Q are taken to be uniform in x and impulsively applied at $t = 0$: $\tau(t) = \tau_0$, $Q(t) = Q_0$ for $t > 0$, while $\tau(t) = Q(t) = 0$ for $t < 0$. These restrictions could be easily lifted.

3. A steady state for upwelling and heating

It is instructive to ask what steady-state solutions may be possible. Setting $\partial/\partial t = 0$ in (5) and (7) gives

$$h_1 u_1 \frac{\partial T_1}{\partial x} = \frac{Q_0}{c\rho} - (T_1 - T_2)\frac{\partial}{\partial x}(h_1 u_1), \quad (8a)$$

$$\frac{1}{2} h_1 \alpha g (T_1 - T_2)\frac{\partial}{\partial x}(h_1 u_1) = m_0 u_*^3 - \frac{1}{2} h_1 \alpha g \frac{Q_0}{c\rho}. \quad (9)$$

The first of these may be rewritten, recalling that T_2 is constant,

$$\frac{\partial}{\partial x}[h_1 u_1 (T_1 - T_2)] = \frac{Q_0}{c\rho}, \quad (8b)$$

or using (1b),

$$\frac{\partial}{\partial x}(h_1 u_1 T_1 + h_2 u_2 T_2) = \frac{Q_0}{c\rho}. \quad (8c)$$

This expresses the simple principle that the divergence of heat flux in the water column must be supplied by surface heating. Eq. (8b) may be integrated to give

$$T_1 - T_2 = -T_* \frac{x/\lambda}{1 - e^{x/\lambda}}, \quad (10)$$

where

$$T_* = -\lambda(Q_0/c\rho)/(\tau_0/f\rho). \quad (11)$$

The arbitrary constant that could be added to the numerator of (10) must be zero to avoid an infinite temperature difference at the coast $x = 0$. For $-x \gg \lambda$, (10) is very nearly

$$T_1 - T_2 = -T_* x/\lambda, \quad (12a)$$

while near $x = 0$ it becomes

$$T_1 - T_2 = T_*. \quad (12b)$$

Eq. (10) means that water upwelled, entrained, and mixed near the coast gets progressively warmer as it moves offshore (for $\tau_0 < 0$) steadily absorbing heat from the sun and atmosphere (for $Q_0 > 0$). The unbounded offshore increase of temperature given by Eqs. (10) or (12a) appears unsettling at first. This behavior is placed in context by considering the approach to steady state from arbitrary initial conditions (Section 4, below). It will be seen that the steady solutions are asymptotic solutions which are approximately attained after a given time t within a region of width ut adjacent to the coast, where u is the normal-to-shore velocity scale. Hence the region of validity of (10) or (12a) is finite and in fact, as will be shown below, joins smoothly to a horizontally uniform region beyond. For winds favorable to upwelling, $\tau_0 < 0$, (10) only gives "sensible" steady-state solutions, that is, statically stable, $T_1 > T_2$, if there is net surface heating, $Q_0 > 0$.

Substituting (10) into (9) and using (1) gives the mixed-layer depth

$$h_1 = h_* \frac{1 - e^{x/\lambda}}{1 - (1 + x/\lambda)e^{x/\lambda}}, \quad (13)$$

where

$$h_* = m_0 u_*^3/(\tfrac{1}{2}\alpha g Q_0/c\rho) \quad [u_* = (|\tau_0|/\rho)^{1/2}], \quad (14)$$

except for a constant factor, is the Monin-Obukhov length. We readily see that

$$h_1 = h_* \quad \text{for} \quad -x \gg \lambda, \quad (15a)$$

$$h_1 = \tfrac{1}{2} h_* \quad \text{at} \quad x = 0. \quad (15b)$$

Again, this solution makes little physical sense unless $Q_0 > 0$. Fig. 2 shows h_1 and $T_1 - T_2$ as functions of x for $\tau_0 < 0$ and $Q_0 > 0$.

That physically sensible upwelling steady states ($\tau_0 < 0$) are possible only for net surface heating ($Q_0 > 0$) can be understood fairly readily in physical terms. If Q_0 is zero, or even worse, negative, the surface mixed layer must get continually cooler due

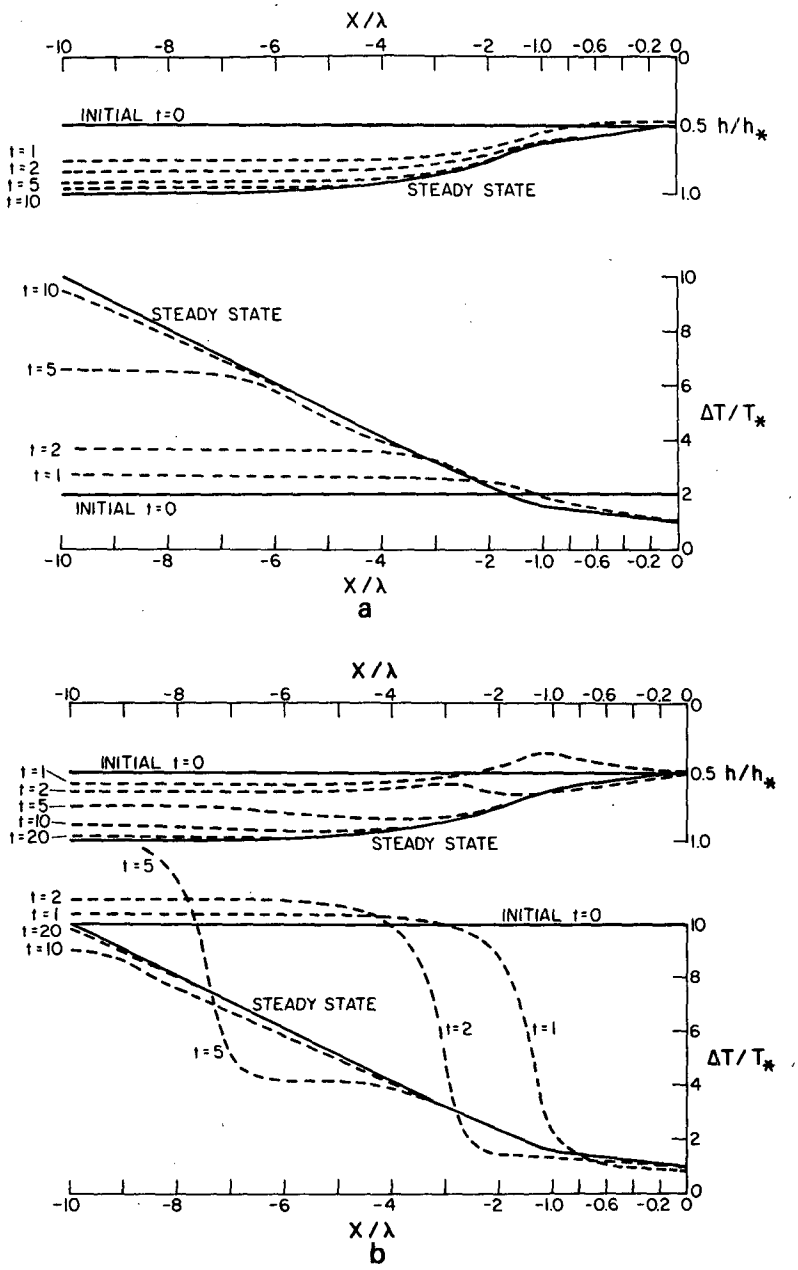

FIG. 2. Time-dependent solutions for mixed layer depth and temperature for an impulsively started wind favorable to upwelling. The heavy lines are the steady state solutions given by Eqs. (10), (13). Note the change in scale at $x/\lambda = -1$.

to both entrainment and sea-to-air exchange, and deeper since both terms on the right of (7) are positive, until it finally attains the bottom layer temperature T_2 or encounters the sea floor. This continually cooler water is pushed offshore by the upwelling-favorable wind in a steadily advancing front. It is clear in such a case that no steady state can be achieved.

The mixed-layer depth beyond the upwelling region is the Monin-Obukhov length, that is, the depth to which turbulent energy input by wind stirring at the rate $m_0 u_*^3$ can penetrate in the face of the stabilizing effects of surface buoyancy flux $\alpha g Q_0/c\rho$. Exponentially little entrainment is happening in this offshore region in the steady state. Toward the coast the mixed-layer depth decreases. Cold water is continually upwelling in this coastal region, and being entrained and mixed into the surface layer at a rate sufficient to balance the air-sea warming and so maintain the steady state.

4. Time-dependent solutions

The steady-state solutions suggest a set of scales to nondimensionalize the time-dependent equations, *viz.*,

$$\left.\begin{aligned} h_1 &= h_* h', \quad T_1 - T_2 = T_* \Delta T' \\ t &= h_*(\tau_0/f\rho\lambda)^{-1} t', \quad x = \lambda x' \\ \tau &= \tau_0 \tau', \quad Q = Q_0 Q', \quad u_1 = \tau_0 (f\rho h_*)^{-1} u_1' \end{aligned}\right\}, \quad (16)$$

where T_*, h_* are given by (11) and (14). The time scale is given by the mixed-layer depth scale h_* divided by the transport divergence (or vertical velocity) scale $\tau_0/f\rho\lambda$. Wind stress τ and surface heat flux Q are considered to be impulsively started at an initial instant $t = 0$. With this scaling equations (5) and (7) become, using (1), (4) and (6) and dropping primes,

$$\frac{\partial h}{\partial t} = \tau e^x + \frac{|\tau|^{3/2} - Qh}{h\Delta T}, \quad (17)$$

$$\left(\frac{\partial}{\partial t} + u_1 \frac{\partial}{\partial x}\right)\Delta T = h^{-1}[Q - h^{-1}(|\tau|^{3/2} - Qh)], \quad (18)$$

where

$$u_1 = (\tau/h)(1 - e^x). \quad (19)$$

Eq. (18) is solved by the method of characteristics,

$$\frac{dx}{dt} = u_1, \quad (20)$$

$$\frac{d}{dt}\Delta T = h^{-1}[Q - h^{-1}(|\tau|^{3/2} - Qh)], \quad (21)$$

where d/dt is the derivative following the motion u_1 in the mixed layer. Eqs. (17), (20) and (21) are then solved as coupled first-order differential equations in time with initial conditions

$$\left.\begin{aligned} x(0; \xi) &= \xi, \quad h(\xi, 0) = h_1(\xi) \\ \Delta T(\xi, 0) &= \Delta T_i(\xi), \quad -\infty < \xi < 0 \end{aligned}\right\}. \quad (22)$$

This is done numerically on a discrete grid of initial positions ξ_n. $x(t; \xi)$ is the family of characteristics of Eq. (18). Note that while on the right sides of (20), (21) x is taken to change with time while ξ remains fixed, on the right side of (17) x remains fixed while ξ varies. A similar method of solution was used by de Szoeke (1980).

Eqs. (17) and (18) contain no explicit dimensionless parameters. If τ and Q are constant in time, then without loss of generality we can set $|\tau| = |Q| = 1$; only variation of the initial conditions can influence the subsequent development of the solutions. Table 1 lists typical magnitudes for dimensional parameters such as wind stress magnitude, surface heating, upwelling region scale, etc., and calculated from them, the depth, temperature (or density), velocity and time scales used in (16). Whatever the scales chosen, the nondimensional solutions to be displayed below can be readily rescaled to accord with any setting of dimensional parameters.

TABLE 1. Typical scale parameters for Oregon upwelling and downwelling events.

	Upwelling 9–14 July 1973	Downwelling 15–23 August 1972
Wind stress τ_0	-1.2 dyn cm^{-2}	0.5 dyn cm^{-2}
Friction velocity u_*	1.1 cm s^{-1}	0.7 cm s^{-1}
Surface heating Q_0	150 W m^{-2}	150 W m^{-2}
Horizontal length scale λ	10 km	10 km
Monin-Obukhov depth h_*	17 m	5 m
Temperature scale T_*	0.3°C	0.8°C
Density scale σ_*	0.06 mg cm^{-3}	0.15 mg cm^{-3}
Time scale $h_* f \lambda u_*^{-2}$	1.7 days	1.1 days
Velocity scale $\tau(\rho f h_*)^{-1}$	-7 cm s^{-1}	10 cm s^{-1}

a. Upwelling with heating

Nondimensional solutions for mixed-layer depth h and temperature difference ΔT as functions of x at various times t are shown in Fig. 2, for conditions favorable for upwelling with $\tau < 0$ and $Q > 0$; specifically $-\tau = Q = 1$.[2] Note the expanded length scale in the range $0 < -x < 1$. In Fig. 2a, initial conditions were $h_i = 0.5, \Delta T_i = 2.0$, while in Fig. 2b they were $h_i = 0.5, \Delta T_i = 10.0$. Figs. 2a and 2b also display the steady-state forms for ΔT and h given by (10) and (13). The tendency of the solutions toward the steady forms with advancing time is clearly evident. For finite time and sufficiently far from the coast, no horizontal gradients have developed, $(\partial/\partial x)\Delta T \approx 0$, and the transport divergence is exponentially small, so that the mixed-layer dynamics is essentially one-dimensional (vertical). Eqs. (17) and (18) become

$$\frac{\partial h}{\partial t} = \frac{|\tau|^{3/2} - Qh}{h\Delta T}, \quad (23)$$

$$\frac{\partial}{\partial t} h\Delta T = Q, \quad (24)$$

where (23) has been used in (18) to obtain (24). This can be directly integrated,

$$h\Delta T = \theta_i + Qt, \quad (25)$$

[2] Having made this choice, however, we retain the notation τ, Q in the following as place markers for the effects of wind and heating.

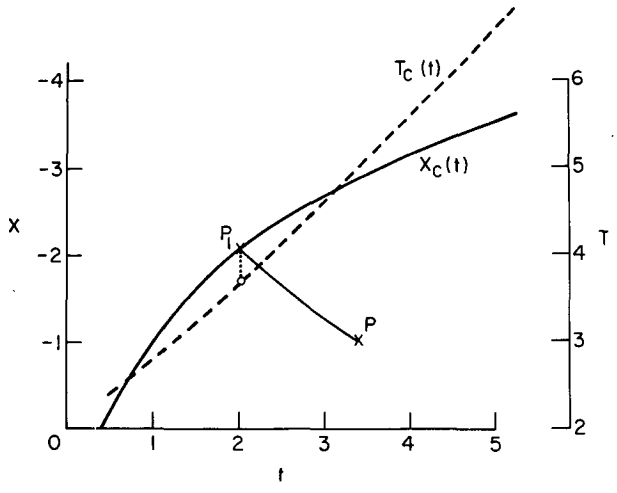

FIG. 3. The boundary x_c inshore of which the Monin-Obukhov depth has been attained as a function of time t for downwelling-favorable winds. Also shown is mixed-layer temperature T_c at (x_c, t) relative to the initial lower layer temperature. Scales are in nondimensional units. Initial conditions are $h_i = 0.5$, $\Delta T_i = 2.0$. The curve P_1P traces the characteristics (32) where P is (x, t) and P_1 is (x_1, t_1).

where $\theta_i = h_i \Delta T_i$ is the initial heat content. Eq. (23) can then be integrated, using (25). The result is

$$h = \frac{|\tau|^{3/2}}{Q} - \frac{\theta_i}{\theta_i + Qt}\left(\frac{|\tau|^{3/2}}{Q} - h_i\right), \quad (26)$$

showing that the mixed-layer depth approaches the local Monin-Obukhov depth $|\tau|^{3/2}/Q$ from above (as long as $Q > 0$, and $h_i < |\tau|^{3/2}/Q$) algebraically for nondimensional times large compared to θ_i/Q. Meanwhile, information about the upwelling region has been propagating offshore at the rate of $-u_1 \approx |\tau|/h \approx Q/|\tau|^{1/2}$, which is unity for $Q = -\tau = 1$, and has reached the nondimensional position $u_1 t$ after time t. This position marks the transition between the upwelling solution, which is tending to the steady solution (10) and (13), and the one-dimensional offshore solution given by (25) and (26).

The contrast between Figs. 2a and 2b is interesting. They differ in their initial conditions, namely that initial heat content $\theta_i = 1$ (a), $\theta_i = 5$ (b). In the latter case a strong temperature front forms at the offshore edge of the upwelling region at $x \approx -1$ in a time of order 1, and then moves offshore with a nondimensional velocity of ~ 1. Shoreward of the front the steady state solution is rapidly approached. The former case does not show such a remarkable front.

This behavior can be understood as follows. In the upwelling region the initial mixed-layer water is immediately advected offshore and replaced by upwelled and warmed lower layer water. Hence, in this region, the initial condition is quickly forgotten and the asymptotic steady-state quickly achieved. This is so even in case (b) where there is an enormous contrast between the initial temperature $\Delta T_i = 10$ and the eventual steady state temperature $\Delta T_\infty \approx 1$. Offshore, the one-dimensional solutions (25), (26) hold, which show that for times earlier than θ_i/Q, h and ΔT change rather little from h_i and ΔT_i. Hence a horizontal temperature contrast or front of order $\Delta T_i - \Delta T_\infty$ develops initially at the boundary between the upwelling region and the offshore one-dimensional mixing region. This contrast is about 9 for case (b) and 1 for case (a). The former is readily discernible in Fig. 2b, while the latter is barely perceptible in Fig. 2a. As the offshore boundary of the upwelling region is advected offshore by the velocity u_1, so too is the associated temperature front. The asymptotic steady state grows linearly with distance offshore, $\Delta T_\infty \approx -x$, in nondimensional units, so that the temperature front is greatly attenuated as it approaches $x = -\Delta T_i$.

b. Downwelling with heating; detrainment

Next consider a situation similar to the previous one except that the direction of the wind is reversed, $\tau = 1$, that is, unfavorable to upwelling; heating still pertains, $Q = 1$. In the offshore region, horizontal gradients are small, so that the tendency toward a one-dimensional mixed layer given by the approximate solution [Eqs. (25) and (26)] still holds. However, the solution in the coastal region is now completely different. For one thing, the direction of propagation of information is the opposite, from offshore toward the coast. The mixed-layer depth increases most rapidly near the coast, where the downwelling velocity is the largest. In fact, the Monin-Obukhov depth (=1 in these nondimensional units) is soon reached at the coast. The boundary x_c inshore of which the Monin-Obukhov depth has been attained migrates offshore with time as shown in Fig. 3. The same figure shows the mixed-layer temperature at this moving boundary as a function of time. These curves depend on the initial conditions, which in the particular case are $h_i = 0.5$ and $\Delta T_i = 2$ (nondimensional) at $t = 0$.

1) DETRAINMENT

Just after the Monin-Obukhov depth is achieved at any location an odd situation occurs, which requires special consideration. If h tends to exceed 1 $(= |\tau|^{3/2}/Q)$, then, from (17) written as

$$h\Delta T\left(\frac{\partial h}{\partial t} - \tau e^x\right) = h\Delta T w_e = |\tau|^{3/2} - Qh, \quad (17')$$

$w_e < 0$ appears to be required for $\Delta T > 0$. This means *detrainment* of water from the mixed layer into the interior, that is, flux of material from the turbulent to the quiescent fluid. We can understand this as follows. The Monin-Obukhov scale is that

depth to which turbulence forced by wind stirring at the surface can penetrate in the face of the stabilizing effect of surface heating. The turbulent water parcel at the bottom of the mixed layer when $h = 1$ is just barely being maintained by the flux of turbulent energy from the surface. In the next instant the downwelling tendency $-\tau e^x$ carries it beyond the marginal depth at which its turbulence can be sustained. Its turbulent kinetic energy is then quickly dissipated and it becomes part of the quiescent lower layer—it is detrained, in other words. This means that the mixed-layer base, taken as marking the boundary between turbulent and quiescent water, retreats from the level of the temperature jump (Fig. 4). The temperature across the mixed-layer base must be continuous, $\Delta T = 0$. This makes the left side of (17') zero, so that to maintain the equality h must remain at 1. But then $\partial h/\partial t = 0$, so that $w_e = -\tau e^x < 0$, i.e., the mixed-layer thickness remains at the Monin-Obukhov depth, while fluid is continually detrained at the downwelling rate $-\tau e^x$ across an interface with no temperature (density) jump. To summarize, once $h = 1$ is attained, (17') is satisfied—unless the external forcing parameters τ, Q change—by requiring separately that

$$\Delta T = 0 \quad \text{and} \quad h = 1. \tag{27a,b}$$

This represents a singular solution to Eq. (17), which straightforward numerical methods will not attain without proper indoctrination. It seems appropriate to term this a *decadent* mixed layer, in contrast to an *active* one.

In the lower layer T_2 is no longer constant [Eq. (6)] as the newly detrained water parcels enter it and move about, carrying with them unchanged the temperature they had as they left the mixed layer. This is expressed by

$$\left(\frac{dT}{dt}\right)_2 = \frac{\partial T_2}{\partial t} + u_2 \frac{\partial T_2}{\partial x} + w_2 \frac{\partial T_2}{\partial z} = 0, \tag{28}$$

where

$$u_2 = \left(\frac{dx}{dt}\right)_2 = -(1 - e^x)/(H - 1), \tag{29a}$$

$$w_2 = \left(\frac{dz}{dt}\right)_2 = -ze^x/(H - 1). \tag{29b}$$

H is the nondimensional total depth of the two layers; $z = 0$ corresponds to the ocean bottom, assumed level. In contrast to the upwelling situation where the homogeneous lower layer played only a passive role so that its depth did not influence the dynamics, in downwelling H influences the development of detrained water property distributions through (29). The temperature T_1 of the mixed layer is governed by a dimensionless form of (5), with (27), so that

$$\left(\frac{dT}{dt}\right)_1 = \frac{\partial T_1}{\partial t} + u_1 \frac{\partial T_1}{\partial x} = Q, \tag{30}$$

where

$$u_1 = \left(\frac{dx}{dt}\right)_1 = 1 - e^x. \tag{31}$$

Eqs. (17)–(19) and/or (27)–(31) can be solved by a combination of numerical and graphical methods. Suppose that water temperature at position (x, z) and time t is desired. First of all integration of Eqs. (17)–(19), with the appropriate initial conditions at $t = 0$, is carried out to time t. If h attains 1 before time t at any position and so becomes decadent,

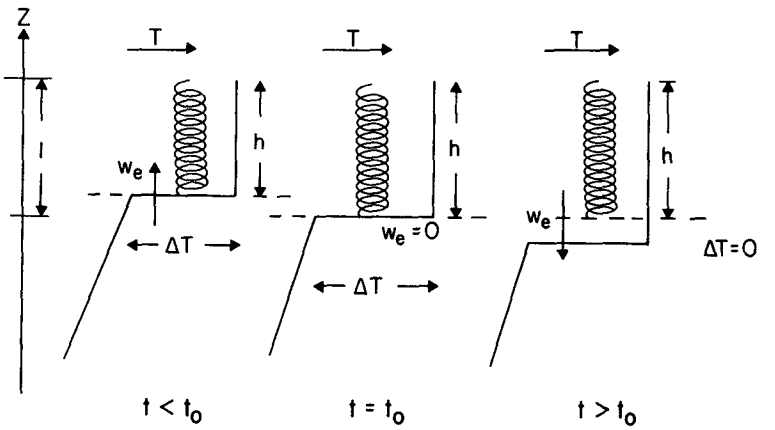

FIG. 4. Schematic diagrams before, at, and after the instant t_0 when the mixed layer attains the Monin-Obukhov depth (=1 in nondimensional units) during downwelling. Before, entrainment is positive, $w_e = \partial h/\partial t - \tau e^x > 0$, $h < 1$, ΔT is nonzero, turbulence ( ) extends to bottom of mixed layer (——). At $t = t_0$, entrainment vanishes, $w_e = 0, h = 1, \Delta T$ is nonzero, turbulence extends to bottom of mixed layer. Slightly afterward, $t > t_0$, $w_e = -\tau e^x < 0$, $h = 1$, detrainment is occurring, turbulence extends only partially through the thermostad; note that $\Delta T = 0$.

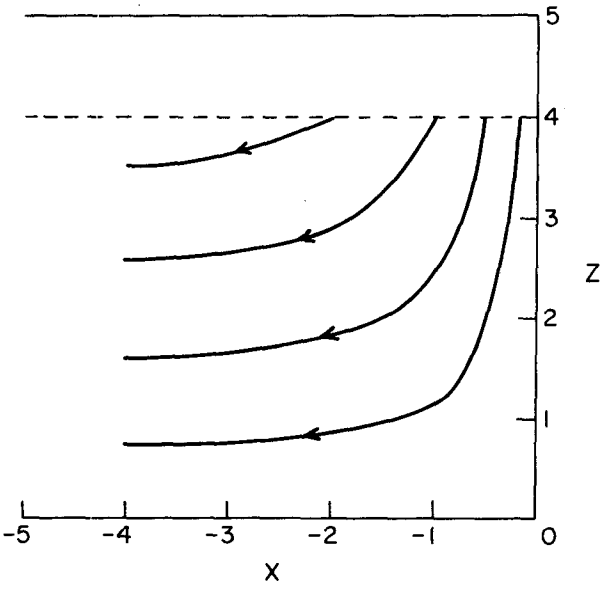

FIG. 5. Trajectories of water parcels detraining from mixed-layer base at $z = H - 1$, from various initial positions x_2.

the right side of (17) is replaced by zero thenceforth at that position or range of positions so that h remains 1 [cf. Eq. (27)]. If the mixed layer is active, $h < 1$, at time t and position x, the temperature at height z is either T_1 or T_2 [= constant, Eq. (6)], according to whether $z \gtrless H - h$. If $h = 1$, the following procedure, based on (27)–(31), is followed. For $z \geq H - 1$, in the decadent mixed layer, Eq. (31) may be integrated to give

$$-x = \ln[1 + (e^{-x_1} - 1)e^{-(t-t_1)}], \qquad (32)$$

which satisfied $x = x_1$ at $t = t_1$. We need to use (32) in the inverted form

$$-x_1 = \ln[1 + (e^{-x} - 1)e^{t-t_1}]. \qquad (32')$$

Mark (x, t) as the point P on Fig. 3. If $h < 1$, active, P will lie above $x_c(t)$ on Fig. 3; if not, decadent, it will lie below, as shown. Plot (32′) as a function of t_1 decreasing from t on Fig. 3 until $x_c(t)$ is intersected; this is the curve PP_1 on Fig. 3. Then the point of intersection P_1 gives (x_1, t_1), which is the position and time at which the water parcel now at (x, t) was last in a marginally active mixed layer. Its temperature $T_1(x_1, t_1) = T_c(t_1)$ at that time t_1 can be determined from Fig. 3. This is used as the initial condition in integrating (30) following the motion to (x, t), *viz.*,

$$T_1(x, t) = Q(t - t_1) + T_c(t_1). \qquad (33)$$

If the point at which the temperature is desired is below a decadent layer, $z < H - 1$, Eqs. (28), (29) must be solved. The solution of (29a) is similar to (32), *viz.*,

$$-x = \ln[1 + (e^{-x_2} - 1)e^{(t-t_2)/(H-1)}], \qquad (34)$$

satisfying $z = z_2$ at $t = t_2$. The trajectory of a water parcel in the lower layer is obtained by solving

$$\frac{dz}{dx} = \frac{dz}{dt}\Big/\frac{dx}{dt} = \frac{ze^x}{1 - e^x}. \qquad (35)$$

This gives

$$z = (H - 1)\frac{1 - e^{x_2}}{1 - e^x}, \qquad (36)$$

which describes, as initial position x_2 is varied, a family of curves emerging from the Monin-Obukhov level at $z = H - 1$ (Fig. 5). Note that as $x < -\infty$

$$z \to z_\infty \equiv (H - 1)(1 - e^{x_2}). \qquad (37)$$

Hence, given (x, z, t), the point of emergence x_2 from the decadent layer can be determined from (36) or Fig. 5, and the time of emergence t_2 from (34). For this time and position, temperature can be determined by the graphical method described above and with Eq. (33) by using (x_2, t_2) for the coordinates of P in Fig. 3. This initial temperature $T_1(x_2, t_2)$ is preserved by the water parcel as it follows the trajectory (35), (36) to position (x, z) at time t, i.e.,

$$T_2(x, z, t) = T_1(x_2, t_2). \qquad (38)$$

2) NUMERICAL SOLUTION

A model calculation for downwelling is displayed in Fig. 6 as a time sequence of panels, each representing an instantaneous section of the temperature (or density) structure normal to shore during a downwelling event. Units are nondimensional [see Eq. (16) and Table 1]. The initial mixed-layer depth and basal temperature difference were $h_i = 0.5$, $\Delta T_i = 2.0$; the initial lower layer relative temperature T_2 was zero everywhere. Fig. 6 clearly shows the attainment of the Monin-Obukhov depth, first at the coast and then advancing offshore, and the consequent detrainment in this region of warm water from the mixed layer and the establishment of a diffuse thermocline beneath the decadent layer. At the leading edge of this stratified region there is a fossil temperature discontinuity, left over from the active phase of the inshore mixed layer (see Fig. 4), that shoals and joins smoothly onto the temperature jump of the active mixed layer offshore. The horizontal surface temperature gradient is very slight at all times. Downwelling with surface heating evidently affords a potent mechanism for establishing subsurface temperature structure. The associated horizontal gradients, like the slope of the active mixed layer interface, can sustain longshore geostrophic shear currents, which are, however, supposed not to play a dynamically active role in a two-dimensional theory such as this.

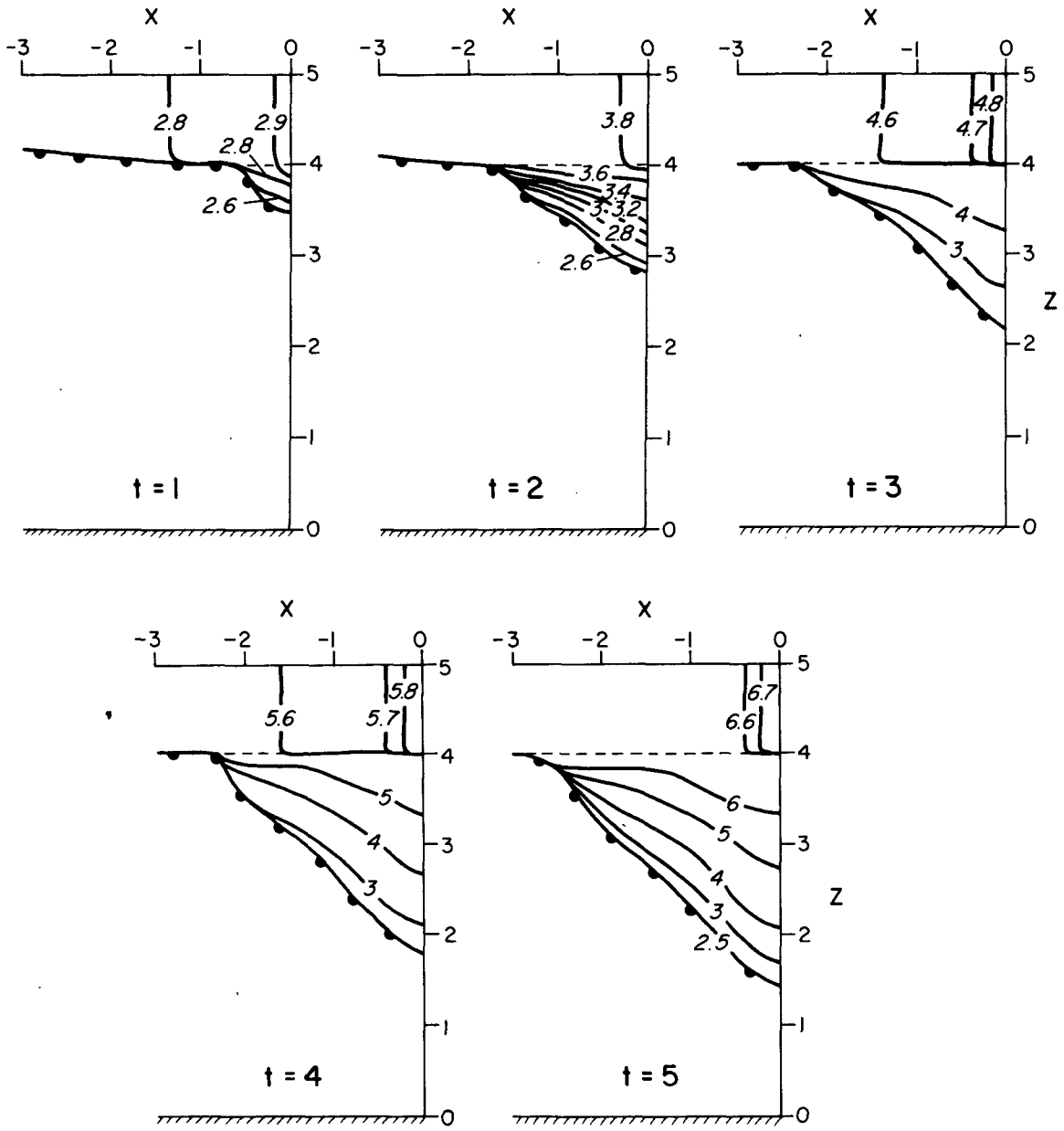

FIG. 6. A time sequence of model sections of temperature in the downwelling case. Note the increasing region of detrained water beneath the decadent mixed layer (dashed line). Solid lines are nondimensional isotherms. In advance of the detrained region and the active mixed layer there is a temperature discontinuity denoted by the warm front symbol. Relative temperature beyond this is zero.

5. Comparison with observations

Our model is quite crude, so that an overly detailed comparison with observations in complicated situations occurring in nature is unwarranted; yet a qualitative comparison ought to be made to confirm or deny whether theoretically expected effects are of the observed order of magnitude. We shall display two examples, one of upwelling, the other of downwelling, both from the Oregon coast, and discuss them in terms of the model.

Fig. 7 shows time series of an upwelling-favorable southward longshore wind stress observed at Newport, Oregon during July 1973, and horizontal sections of the difference of bottom to surface density and mixed layer depth—the latter judged on a 0.1 deg C difference criterion—, taken from a series of repeated *CTD* sections transverse to the continental

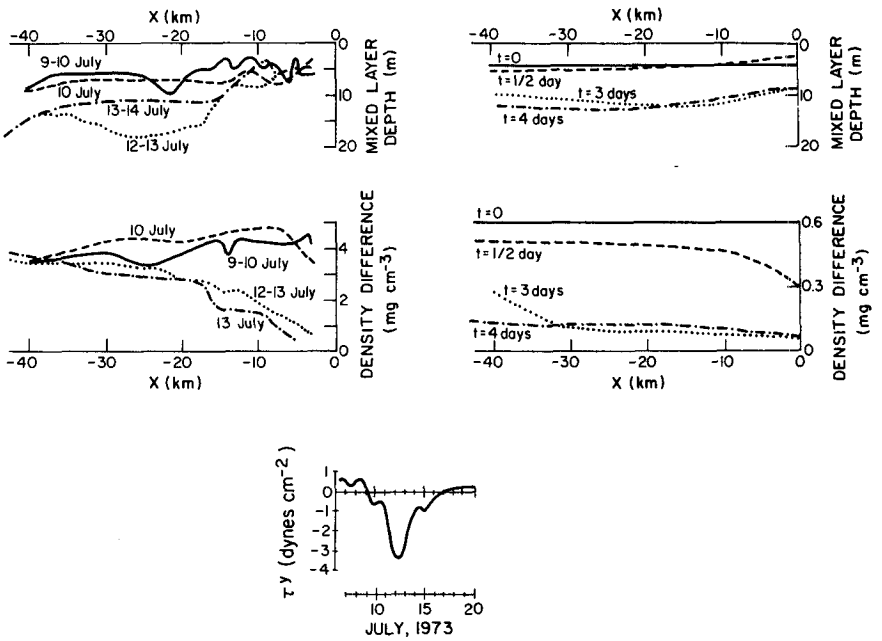

FIG. 7. Mixed-layer depth, bottom to surface σ_t difference versus offshore distance from four CTD sections across the continental shelf at Newport, Oregon, during July 1973 and model comparisons for the parameter choice in Table 1. Longshore wind stress from a shore station at Newport is also shown.

shelf in the period 9–14 July 1973 (Huyer and Gilbert, 1974). The bottom density is nearly constant in both space and time at $\sigma_t = 26.7$ mg cm^{-3} during the entire upwelling event. It contrasts strongly with the surface σ_t which initially (9–10 July) varied from 22 mg cm^{-3} at the coast to 23 mg cm^{-3} at 40 km offshore. After the wind peaked, (13–14 July) it varied between $\sigma_t \doteq 26.0$ and 26.5 mg cm^{-3} at the coast, increased approximately linearly at 0.2 mg cm^{-3} km^{-1} out to 20 km offshore, then rather more slowly out to 40 km where surface conditions changed little during the entire upwelling event. The estimate of mixed-layer depth, though extremely variable in space and time and undoubtedly strongly aliassed by internal motions, hovered in a shallow range of 3–7 m between the coast and 13 km for the entire duration. Offshore it increased from 5–7 m before the wind peak, to 10–15 m after.

To compare with the model, we chose to use a mean wind stress $\tau^y = -1.2$ dyn cm^{-2} and a surface energy exchange rate $Q = 150$ W m^{-2}. The surface energy exchange rate is the 10-year mean summertime exchange rate off Oregon obtained by Lane (1965). Moored and shipboard radiometer measurements of Reed and Halpern (1975) off Oregon in July and August, 1973 are consistent with Lane's (1965) climatological value. Solar radiation dominates the summertime heat transfer. For this choice of parameters the Monin-Obukhov depth is 17 m and the temperature scale T_* is 0.3°C (corresponding to a density scale of 0.06 mg cm^{-3}). To compare with the data shown in Fig. 7, we chose an initial mixed-layer depth of 4 m and an initial density difference of 0.6 mg cm^{-3}. In the model the mixed-layer depth initially shallows to 3 m near the coast and subsequently deepens to 8 m. Offshore the mixed layer deepens to 13 m at a rate of 2 m day^{-1}. The depth of the mixed layer in the model is qualitatively similar to the observations. Disagreement between the model and the observations is larger in the density difference between the mixed layer and the fluid below. In both the model and the observations, the density difference near the coast drops rapidly toward a small value. However, the model develops a wider zone of small density difference (cold water in the mixed layer) bounded by a sharp front (Fig. 2b). This sharp front does not develop in the observations, rather the density difference increases almost linearly out to 40 km corresponding to a nearly linear density gradient near the surface. This linear gradient resembles the steady-state solution shown in Fig. 2b. Possibly longshore advection neglected by the model prevents the development of an upwelling front.

Fig. 8 displays an instance of coastal downwelling off Newport, Oregon during August 1972 (Curtin and Mooers, 1974). To be precise, there are two instances of significant southerly downwelling-favorable wind, each lasting about one day, one on 17 August, the other on 21–22 August. Density sec-

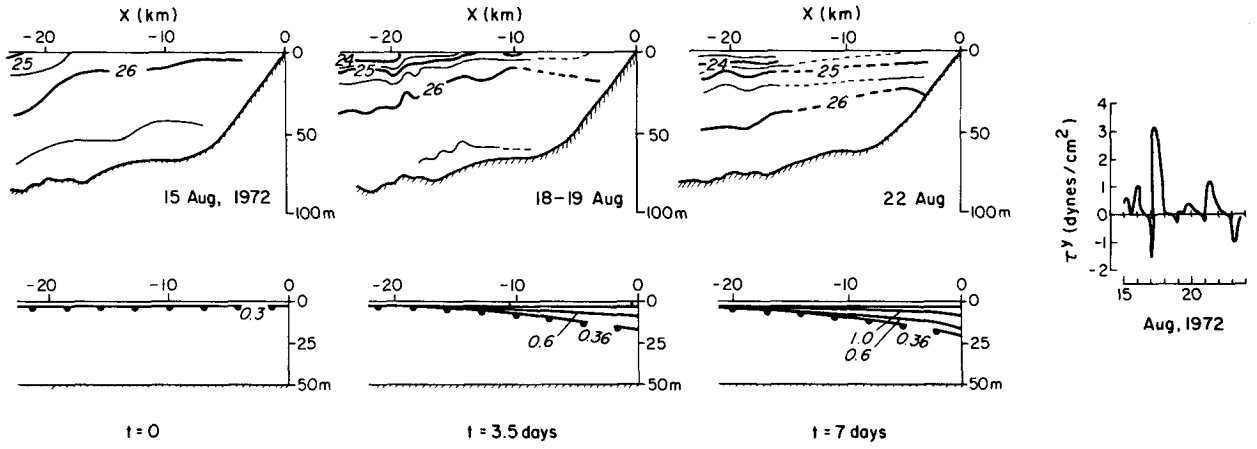

FIG. 8. σ_t sections off Newport, Oregon, during August 1972. Longshore wind stress is shown. Accompanying panels display dimensional versions of the model results for relative density (cf. Fig. 6) for the parameter choice of Table 1.

tions before, between, and after these events are shown. Also shown are model comparisons similar to Fig. 6 at times corresponding roughly to the elapsed time between the sections: time, horizontal and vertical space, and relative density dimensions on these panels correspond to the parameter settings $\tau = 0.5\,\text{dyn cm}^{-2}, Q = 150\,\text{W m}^{-2}, \lambda = 10\,\text{km}$. [See Eq. (16) for the dimensional scale conversions.] The data show a general downward motion of mid-depth isopycnals, best illustrated by the 26.0 mg cm^{-3} surface, and an onshore motion of shallow isopycnals, such as the 24.0, 25.0 mg cm^{-3} surfaces. Before 15 August a fairly complex horizontal and vertical stratification existed, so that it is no surprise that the model, initially uniform horizontally and with a density contrast of only 0.3 mg cm^{-3}, does not mimic the evolution of the details in the data. Still, at 10 km offshore the bottom-to-top density contrast increases from 0.6 to 1.6 mg cm^{-3} while the model shows an increase from 0.36 to 1.1 mg cm^{-3}. The similarity in motion between the 26.0 mg cm^{-3} isopycnal and the density difference front inshore of 10 km is remarkable. The model does not show the onshore motion of shallow isopycnals indicated in the observations. Again, longshore advection may be responsible for this discrepancy.

Although it has been convenient to speak of 'temperature' in the formulation of the model, we could as easily have framed it in terms of density. A distinction must be made in nature, however, where salinity can independently influence density distribution. This is especially striking off Oregon where temperature inversions are frequently observed because of the compensating stabilization by the halocline (Huyer and Smith, 1974). Applying our solutions to such a situation, then, model 'temperature' ought to be identified with density, as has been done above.

6. Discussion and conclusions

On balance, the qualitative features and scales predicted by the model accord reasonably with observation. This is in spite of the slight resemblance of the actual wind stress to a wind impulsively started, then constant. A similar remark can be made for surface heating, the far greater complexity of density structure below the mixed layer than can be rendered by a two-layer model, the neglect of topography and its effect on the dynamics of the lower layer, and the neglect of any longshore nonuniformities in nature which would bear on the interpretation of the observations. To stress again the merits of the model: only a mixing mechanism can satisfactorily account—saving an explanation relying on longshore advection—for the increase in density at the surface commonly observed during upwelling despite net air-to-sea heat exchange.

Contrasting the data of Figs. 7 and 8 illustrates the asymmetry between upwelling and downwelling in nature. A tendency toward the homogenization of the onshore water columns occurs during upwelling, with the opposite during downwelling, a well-defined surface mixed layer during upwelling—though with considerable horizontal structure—and a thin and indistinct mixed layer during downwelling, especially near the coast. Both tendencies are well represented in the model runs. These asymmetries, moreover, must be a reflection of the adiabatic, irreversible and nonlinear character of the dynamical processes occurring in nature. Minimally, a dynamical model that can reproduce these features must possess the same characteristics.

Pattullo *et al.* (1969) computed the heat content of the upper 100 m off Oregon for the period 1962–65, and analyzed variability on-, off- and alongshore, and seasonally and interannually. They found that

(i) heat content increases offshore between July and September, while (ii) it is fairly uniform normal to shore during the rest of the year, and (iii) there is little alongshore heat content variability. July through September is generally the season of upwelling in Oregon (Mooers *et al.*, 1976). Point (i) corroborates the offshore increase of the model mixed-layer temperature during upwelling and supports the observations shown in Fig. 7. Point (ii) corroborates our downwelling model results (Figs. 6 and 8). Point (iii) lends support to the simplifying assumption of alongshore uniformity.

The role of surface heating in the model must be stressed. Without it, the steady upwelling state cannot exist; time-dependent upwelling solutions, which seem to 'forget' their initial conditions very readily and strive towards the steady state, would be very different. Similarly, during downwelling the decadence of the mixed layer, detrainment, and subsurface thermocline establishment depend intimately on net sea-air heat exchange. The effect of heating has been a neglected feature in most upwelling models, or, if not neglected, then not fully appreciated (Pedlosky, 1974; Thompson, 1978). It is relevant to remark, in this context, that coastal upwelling is frequently a summertime phenomenon, for example in Oregon, Northwest Africa and Peru.

On the other hand, Bryden *et al.* (1980) obtained an approximate balance of the Oregon coastal heat budget in which "the offshore heat transport by the mean circulation is balanced by a combination of onshore eddy heat flux, alongshore variation of heat transport by the mean alongshore currents, radiative heat gain by the coastal water, and cooling of the coastal waters." Radiative heat gain is a significant, though not predominant, part of this balance. This contrasts with our two-dimensional model in which the heat balance must be between air-sea exchange, offshore transport and local storage. Three-dimensionality allows a degree of freedom which may vitiate some of the results of the model. However, Bryden *et al.*'s Oregon heat budget is balanced over a 55-day average. Over shorter time scales ($\sim$10 days) of the order of a wind event, a different ordering of the budget terms may pertain, and two-dimensionality be more closely approximated.

Numerous oversimplifications in the formulation of the model have already been noted. Another is the heuristic nature of the proposed momentum dynamics. Ekman transport in the surface layer is attenuated to zero in a baroclinic Rossby radius of the coast. A consistent and tractable treatment of the momentum balance that admits such features is possible, we believe, although at the cost of greater computational effort. It will be explored in a subsequent paper. There is also the question of the appropriate dynamics of the lower layer flow, which is assumed uniform in the vertical throughout this paper. On the proper treatment of this the models of Pedlosky (1978a,b), for example, provide guidance.

Our final warning concerns the unsubstantiated dominance of wind stirring in coastal mixing and its particular parameterization in Eq. (7). Alternatives include internal shear mixing (Pollard *et al.*, 1973) and bottom turbulence generated by strong flows, such as tidal currents in shallow seas (Simpson *et al.*, 1978). Elaborations of the KT parameterization are possible that take these effects into account.

Acknowledgments. This research was sponsored by the National Science Foundation under Grant OCE 79-25396, and by the Office of Naval Research under Contract N000174-79-C-0004, Project NR 083-102.

REFERENCES

Allen, J. S., 1973: Upwelling and coastal jets in a continuously stratified ocean. *J. Phys. Oceanogr.*, **3**, 245–257.

——, 1980: Models of wind-driven currents on the continental shelf. *Annual Review of Fluid Mechanics*, Vol. 12, Annual Reviews, Inc., 389–433.

Bryden, H. L., D. Halpern and R. D. Pillsbury, 1980: Importance of eddy heat flux in a heat budget for Oregon coastal waters. *J. Geophys. Res.*, **85**, 6649–6653.

Curtin, T. B., and C. N. K. Mooers, 1974: Coastal Upwelling Experiment I: Hydrographic data report. CUEA Data Rep. No. 3, 69 pp.

Davis, R. E., R. de Szoeke, D. Halpern and P. Niller, 1981a: Variability in the upper ocean during MILE. Part I: The heat and momentum balances. *Deep-Sea Res.* (in press).

——, —— and P. P. Niiler, 1981b: Variability in the upper ocean during MILE. Part II: Modelling the mixed layer response. *Deep-Sea Res.* (in press).

Denman, K. L., 1973: A time-dependent model of the upper ocean. *J. Phys. Oceanogr.*, **3**, 173–184.

——, and M. Miyake, 1973: Upper layer modification at Ocean Station Papa: observations and simulation. *J. Phys. Oceanogr.*, **3**, 185–196.

de Szoeke, R. A., 1980: On the effects of horizontal variability of wind stress on the dynamics of the ocean mixed layer. *J. Phys. Oceanogr.*, **10**, 1439–1454.

——, and P. B. Rhines, 1976: Asymptotic regimes in mixed-layer deepening. *J. Mar. Res.*, **34**, 111–116.

Ekman, V. W., 1905: On the influence of the earth's rotation on ocean currents. *Arkiv. Math. Astron. Fys.*, **2**, 1–52.

Greenspan, H. P., 1968: *The Theory of Rotating Fluids*. Cambridge University Press, 327 pp.

Hurlburt, H. E., and J. D. Thompson, 1973: Coastal upwelling on a β-plane. *J. Phys. Oceanogr.*, **3**, 16–32.

Huyer, A., and W. E. Gilbert, 1974: Coastal Upwelling Experiment hydrographic data report. Oregon State University Data Rep. No. 59, Ref. 74–8, 102 pp.

——, and R. L. Smith, 1974: A subsurface ribbon of cool water over the continental shelf off Oregon. *J. Phys. Oceanogr.*, **4**, 381–391.

Johnson, W. R., J. C. Van Leer and C. N. K. Mooers, 1976: A cyclesonde view of coastal upwelling. *J. Phys. Oceanogr.*, **6**, 556–574.

Kraus, E. B., and J. S. Turner, 1967: A one-dimensional model of the seasonal thermocline: II. The general theory and its consequences. *Tellus*, **19**, 98–106.

Kundu, P. K., 1976: An analysis of inertial oscillations observed near Oregon coast. *J. Phys. Oceanogr.*, **6**, 879–893.

——, 1980: A numerical investigation of mixed-layer dynamics. *J. Phys. Oceanogr.*, **10**, 220–236.

Lane, R. K., 1965: Climate and heat exchange in the oceanic region adjacent to Oregon. Ph.D. thesis, Oregon State University, 115 pp.

Mellor, G. L., and P. A. Durbin, 1975: The structure and dynamics of the ocean mixed layer. *J. Phys. Oceanogr.*, **5**, 718–728.

Mooers, C. N. K., C. A. Collins and R. L. Smith, 1976: The dynamic offshore of the frontal zone in the coastal upwelling region off Oregon. *J. Phys. Oceanogr.*, **6**, 3–21.

Niiler, P. P., 1975: Deepening of the wind-mixed layer. *J. Mar. Res.*, **33**, 405–422.

——, and E. B. Kraus, 1977: One-dimensional models of the upper ocean. *Modelling and Prediction of the Upper Layers of the Ocean*, E. B. Kraus, Ed., Pergamon Press, 153–172.

Pattullo, J. G., W. V. Burt and S. A. Kulm, 1969: Oceanic heat content off Oregon: its variations and their causes. *Limnol. Oceanogr.*, **14**, 279–287.

Pedlosky, J., 1974: Longshore currents and the onset of upwelling over bottom slope. *J. Phys. Oceanogr.*, **4**, 310–320.

——, 1978a: An inertial model of steady coastal upwelling. *J. Phys. Oceanogr.*, **8**, 171–177.

——, 1978b: A nonlinear model of the onset of upwelling. *J. Phys. Oceanogr.*, **8**, 178–187.

Pingree, R. D., and D. K. Griffiths, 1978: Tidal fronts on the shelf seas around the British Isles. *J. Geophys. Res.*, **83**, 4615–4622.

Pollard, R. T., P. B. Rhines and R. O. R. Y. Thompson, 1973: The deepening of the wind-mixed layer. *Geophys. Fluid Dyn.*, **4**, 381–404.

Price, J. F., C. N. K. Mooers and J. C. Van Leer, 1978: Observation and simulation of storm-induced mixed layer deepening. *J. Phys. Oceanogr.*, **8**, 582–599.

Reed, R. K., and D. Halpern, 1975: Insolation and net long-wave radiation off the Oregon coast. *J. Geophys. Res.*, **80**, 839–844.

Rossby, C. G., 1938: On the mutual adjustment of pressure and velocity distributions in certain simple current systems, II. *J. Mar. Res.*, **1**, 239–263.

Rouse, H., and J. Dodu, 1955: Turbulent diffusion across a density interface. *La Houille Blanche*, **10**, 522–532.

Simpson, J. H., C. M. Allen and N. C. G. Morris, 1978: Fronts on the continental shelf. *J. Geophys. Res.*, **83**, 4607–4614.

Sverdrup, H. U., M. W. Johnson and R. H. Fleming, 1942: *The Oceans*. Prentice-Hall, 1087 pp.

Thompson, J. D., 1978: Role of mixing in dynamics of upwelling systems. *Upwelling Ecosystems*, R. Boje and M. Tomczak, Eds., Springer-Verlag, 203–222.

Turner, J. S., 1968: The influence of molecular diffusivity on turbulent entrainment across a density interface. *J. Fluid Mech.*, **33**, 639–656.

Yoshida, K., 1955: Coastal upwelling off the California coast. *Rec. Oceanogr. Works Japan*, **2**, 8–20.